





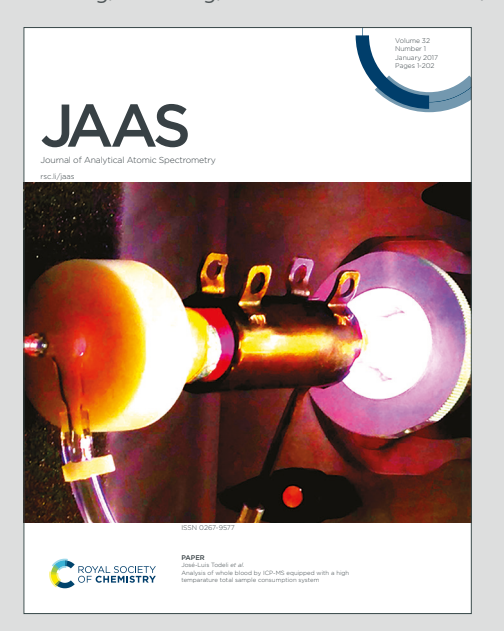
View Article Online

View Journal

Journal of Analytical Atomic Spectrometry

Accepted Manuscript

This article can be cited before page numbers have been issued, to do this please use: X. Zheng, X. Chen, W. Ding, Y. Zhang, S. Charin and Y. Gérard, *J. Anal. At. Spectrom.*, 2022, DOI: 10.1039/D2JA00078D.



This is an Accepted Manuscript, which has been through the Royal Society of Chemistry peer review process and has been accepted for publication.

Accepted Manuscripts are published online shortly after acceptance, before technical editing, formatting and proof reading. Using this free service, authors can make their results available to the community, in citable form, before we publish the edited article. We will replace this Accepted Manuscript with the edited and formatted Advance Article as soon as it is available.

You can find more information about Accepted Manuscripts in the <u>Information for Authors</u>.

Please note that technical editing may introduce minor changes to the text and/or graphics, which may alter content. The journal's standard <u>Terms & Conditions</u> and the <u>Ethical guidelines</u> still apply. In no event shall the Royal Society of Chemistry be held responsible for any errors or omissions in this Accepted Manuscript or any consequences arising from the use of any information it contains.



ġ Zġ

Published on 2012 April 2012 Apri

Gérard^b

•

Revised manuscript for JAAS

^aDepartment of Earth and Environmental Sciences, University of Minnesota—Twin Cities, Minneapolis, MN 55455, USA. E-mail: zhengxy@umn.edu

^bNu Instruments, Unit 74 Clywedog Road South Wrexham Industrial Estate, Wrexham LL13 9XS, United Kingdom

[†] Electronic supplementary information (ESI) available.

ġ Zġ

10:25:57:02/275:07

- Twin Cities on 2

- TO STATE TO THE TOTAL THE TOTAL TO STATE TO THE TOTAL TO THE TOTAL THE TOT

Stable potassium (K) isotopes (41K/39K) have shown great promise as novel chemical tracers for a wide range of bio-, geo-, and cosmo-chemical processes, but high precision stable K isotope analysis remains a challenge for plasma source mass spectrometry due to intense argonrelated interferences produced directly from argon plasma. Here we provide an assessment on the analytical figures of merit of a new generation collision-cell equipped multi-collector inductively coupled plasma mass spectrometer (MC-ICP-MS), Sapphire from Nu Instruments, for K isotope analysis based on our extensive tests over a duration of ~8 months. Because use of helium and hydrogen as collision/reaction gases can reduce argon-related interferences to negligible levels at optimal flow rates, the collision-cell mode can operate at low mass resolution during K isotope analysis, providing >2 orders of magnitude higher K sensitivity (>1000 V per µg mL⁻¹ K), as compared to the widely used "cold plasma" method, and the capability for direct ⁴⁰K measurement. One challenge of the collision/reaction cell analysis on Sapphire is its higher susceptibility to matrix effects, requiring effective sample purification prior to analysis. Also, the collision-cell mode on Sapphire shows a pronounced effect associated with concentration (or ion intensity) mismatch between the sample and the bracketing standard during analysis, and this effect may not be fully eliminated through conventional concentration matching practice. Instead, we developed a correction method for this concentration/ion intensity mismatch effect. Our method reduces the burden to the operator and increases sample throughput. This method allows for accurate K isotope analysis with an intermediate precision of ≤ 0.05 ‰ (2SD) to be routinely achieved using the collision cell on Sapphire, representing a major advance to stable K isotope analysis.

ġ Zġ

1. Introduction

Potassium (K) participates in a wide range of geo-, bio-, and cosmo-chemical processes. As an incompatible element, K is enriched in the crust (~2 % wt in K₂O) and comparably depleted in the mantle (~250 µg g⁻¹ K). ¹⁻⁴ This marked contrast in concentrations makes K a useful indicator for studying material-exchange processes between the crust and the mantle, such as volcanism, subduction, and metasomatism.⁵⁻⁸ Potassium is a trace constituent in the core with estimated concentrations ranging from a few to up to $\sim 250 \mu g g^{-1}$, 9-12 and its precise abundance, which remains debated, has implications for the geodynamo and heat flow of the Earth due to the energy produced by radioactive decay of ⁴⁰K. Because K primarily resides in silicate minerals rather than carbonates, its geochemical cycle in surface environments is intimately linked to silicate weathering and possible formation of authigenic clays in the ocean – the two critical processes that work in tandem in maintaining the general stability of the global carbon cycle (hence climate) and ocean chemistry over the geological timescale. 13-15 In the biological realm, K is an essential nutrient required by both plants and animals, including humans, to maintain many critical physiological functions, 16-18 such as enzyme activation and protein synthesis. Furthermore, because of its moderate volatility with a 50 % condensation temperature (T₅₀) of ~1000 Kelvin, ^{19, 20} K has useful bearing for key evaporation and condensation processes pertinent to formation of the Earth and other planetary bodies.²¹⁻²⁴ Improved knowledge on K cycling and its role(s) in these low- and high-temperature processes has significant implications for the understanding of the Earth system (including various forms of life) and other planetary bodies. Potassium has one naturally occurring radioactive isotope (40K) with a long half-life of

 1.249×10^9 years, ²⁵⁻²⁷ and two stable isotopes (³⁹K and ⁴¹K). Although the use of radioactive

decay of ⁴⁰K as a geochronometer underpinning the K-Ar and Ar-Ar dating techniques has been successful, 25, 28 application of stable K isotope ratios (41K/39K) to study of the K cycle has long been deterred by analytical difficulties. Early attempts to analyze 41K/39K ratios used thermal ionization mass spectrometry (TIMS), and they were only able to achieve an external precision of ~ 1 %...²⁹⁻³¹ Because the conventional double spike method is not applicable to K that has only three isotopes, robust mass bias correction pertinent to study of natural mass-dependent ⁴¹K/³⁹K variations is challenging during TIMS measurement, although several techniques, such as internal normalization, total evaporation, and incipient emission TIMS, can produce precise ⁴¹K/³⁹K data appropriate for different purposes, such as quantification of ⁴¹K excesses or absolute K isotope abundances.³²⁻³⁴ A revised double spike method applicable to three-isotope systems, in principle, can improve 41K/39K analysis by TIMS, 35 but such application has yet to be demonstrated for K. Secondary ionization mass spectrometry (SIMS) has also been applied to analyze stable K isotopes, but the best precision reported in literature was ~0.5 \%. 23, 36 This precision was sufficient to study large 41K/39K variations in some extraterrestrial samples but could not resolve ⁴¹K/³⁹K variations in terrestrial samples.³⁶

Recent studies have shown that multi-collector inductively coupled plasma mass spectrometry (MC-ICP-MS) can achieve a precision of better than ~0.20 ‰ (2SD) for ⁴¹K/³⁹K measurements. ³⁷⁻⁴⁰ This improved precision has quickly led to discoveries of natural ⁴¹K/³⁹K variations in many terrestrial and extraterrestrial samples that were not resolvable in the past, shedding new light on a wide range of critical processes ranging from formation of the moon to silicate weathering. ⁴¹⁻⁶⁰ The current understanding of stable K isotopes has been summarized in a recent review. ⁶¹ Despite being possible, MC-ICP-MS analysis of K isotopes suffers from major challenges associated with intense Ar-related interferences arising directly from the argon

ġ Zġ

plasma, for example, argon hydride (40 ArH⁺) on 41 K⁺. One approach that overcomes these interferences relies on high mass resolution capability available on mainstream MC-ICP-MS instruments, $^{39, 62-66}$ often coupled with a reduced radio frequency (RF) power and an increased distance between the torch and the instrument interface (i.e., the so-called "cold plasma") to further suppress Ar-related ions during the analysis. Although this approach has proven successful, it typically sacrifices >90 % K sensitivity in exchange of sufficient resolving power to resolve Ar hydride interferences. This makes it challenging to analyze low K samples of potentially high science value, such as certain meteorites, carbonates, and mantle rocks.

A collision/reaction cell coupled with MC-ICP-MS represents the other approach that has been used for K isotope analysis.^{67, 68} High precision K isotope measurements with a precision of better than 0.2 % (2SD) were first realized on the Micromass *IsoProbe* MC-ICP-MS,^{37, 38} which had been the only MC-ICP-MS instrument equipped with a collision cell on the market for a few decades until recently. Because Ar-based interferences on K isotopes can be removed in a collision/reaction cell, this approach allows for analysis at low mass resolution. In principle, this should lead to a significant increase in K sensitivity (hence reduced sample consumption) and increased precision. However, given the fact that the *IsoProbe* was an instrument manufactured over 20 years ago, its analytical benefits were not as evident as one would expect, as compared to "cold plasma" measurements made on newer generations of MC-ICP-MS instruments. In addition, the *IsoProbe* was discontinued long time ago, limiting the access to the collision/reaction cell method for K isotope analysis.

The new generation of collision cell equipped MC-ICP-MS instruments has become available recently,⁶⁹⁻⁷³ and these instruments include *Sapphire* from Nu Instruments, *Proteus* and its successor, the upcoming collision cell version of *Neoma*, from Thermo Scientific. The

ġ Zġ

increasing availability of these new instruments in the community has revived the interest in applying the collision/reaction cell to analysis of K isotopes. 70, 72, 74 as well as several other isotope systems that can benefit from the cell, such as calcium (Ca) and strontium (Sr). 71, 73 Recent studies have demonstrated the improved capability of one of these new instruments. Sapphire MC-ICP-MS from Nu Instruments, for high precision stable K isotope analysis. 70, 72 However, assessment of the figures of merit of this new instrument remains limited because of the short time span since the official launching of this instrument to the market. Here, we provide our assessment on the strengths and limitations of Sapphire MC-ICP-MS for stable K isotope analysis, based on more extensive tests over a longer period (i.e., ~8 months) relative to previous studies. In particular, in light of recent reports on pronounced influence of concentration mismatch between the analyte and the bracketing standard on isotope ratios measured by the collision cell on Sapphire MC-ICP-MS, ⁷⁰⁻⁷² we paid special attention to this effect and provided a method that permits robust correction for the effect of moderate concentration mismatch. Using this correction method, we achieved a precision of $\leq 0.05 \%$ (2SD) on ${}^{41}\text{K}/{}^{39}\text{K}$ measurements using the collision cell on Sapphire MC-ICP-MS. It is anticipated that our correction method can be applied to the analysis of many other stable isotope ratios on Sapphire or other MC-ICP-MS

2. Experimental section

instruments.

2.1 Nomenclature, reagents, and materials

Stable K isotope ratios, ${}^{41}\text{K}/{}^{39}\text{K}$, are expressed by the conventional δ -notation:

$$\delta^{41} K = \left(\frac{{}^{41}K/{}^{39}K_{sample}}{{}^{41}K/{}^{39}K_{NIST\ SRM\ 3141a}} - 1\right) \times 1000$$

ġ Zġ

used interchangeably in the literature to describe the closeness of agreement between measurement results, but the strict use of these terms depends on specific conditions. Based on the recommendations from International Organization for Standardization (ISO 5725-3:1994, https://www.iso.org/obp/ui/#iso:std:iso:5725:en), "repeatability" should be used when all factors related to the measurement (e.g., operator, equipment, environment, and reagents) remain constant and do not contribute to the observed measurement variability, whereas "reproducibility" should be used when all factors related to the measurement vary and contribute to the measurement variability. If only some but not all factors vary, the precision should be referred to as "intermediate precision". Measurement of the same rock reference material but from different digestions in a laboratory over a relatively long period of time is one example where "intermediate precision" should be used. ⁷⁶ We follow these definitions in this study to promote accurate scientific communications, and the "precision" reported for our results refers to "intermediate precision" unless specified otherwise.

A suite of pure K solutions and geological reference materials were used for various tests in this study. Pure K solutions included: NIST SRM 3141a, NIST SRM 193, NIST SRM 918b, NIST SRM 999b, and a pure K solution purchased from High-Purity Standards (referred to as "UMN-K"). NIST SRM 3141a was used as the bracketing standard during our analysis. UMN-K has been routinely analyzed in our lab as one of the data quality control standards. This solution is valuable because it has a high δ^{41} K value of 0.44 ‰ (\pm 0.05 ‰, 2SD) (ESI Table S1). When it is analyzed together with seawater and various rock standards, data accuracy across a wider

δ⁴¹K range can be monitored. Geological reference materials analyzed in this study included: natural seawater collected from 500 m at the SEATS site in the South China Sea,⁷⁷ and four USGS rock standards covering mafic to felsic compositions (BHVO-2, BCR-2, AGV-2a, GSP-2).

Sample preparation was performed in a class-100 (ISO Class 5 equivalent) trace-metal free clean lab in the Department of Earth and Environmental Sciences, University of Minnesota-Twin Cities. High purity reagents, including various acids and Milli-Q water (18.2 m $\Omega \cdot$ cm), were used throughout this study. OptimaTM grade hydrofluoric acid (HF) was purchased from Fisher Scientific. Nitric acid (HNO₃) and hydrochloric acid (HCl) were either directly purchased as OptimaTM grade acids or distilled in house using trace metal grade acids and Savillex Teflon DST-1000 acid purification systems in our clean lab. House-distilled HNO₃ and HCl had similar metal blanks as compared to OptimaTM acids. Samples were processed in Savillex Teflon vials that were subject to intense acid cleaning prior to use. USGS rock standards were dissolved in mixed concentrated HNO₃ and HF (1:5, v/v) on a Teflon-coated graphite hotplate at ~150°C for a few days before evaporated to dryness, and the samples were then re-dissolved fully in HCl. Typically, ~5-50 mg rock powders were dissolved each time. Because it is well-known that insoluble fluorides may form during silicate dissolution using HF, 78 sample solutions after dissolution were centrifuged and then examined carefully to ensure the absence of visible gellike fluoride precipitates before further processing for K isotope measurement. It was previously observed that K did not partition perceptibly into fluoride precipitates, even fluorides formed during HF dissolution of silicates.⁷⁹ Therefore, we conclude that our dissolution protocol was unlikely to introduce biases to K isotope ratio measurements for rock reference materials.

ġ Zġ

2.2 Ion exchange chromatographic separation

Except for pure K solutions, geological reference materials were processed through chromatographic columns to purify K prior to isotope analysis. Potassium was separated from sample matrix elements using Bio-Rad AG 50W-X8 cation exchange resin (H⁺ form, 200-400 mesh) packed in Bio-Rad Poly-Prep columns (2 mL resin bed). Separation was achieved using 0.4 mol L⁻¹ HCl, and the detailed elution protocol was provided in Table 1. A two-stage purification using the same elution protocol was required to achieve optimal matrix levels needed for accurate K isotope analysis by the collision/reaction cell (details in Section 3.3.2). Chromatographic column yield is estimated to be nearly quantitative (99% + 5%, n = 15) based on processing of known quantities of K (as pure K solutions) through column separation and subsequent determination of the amount of K recovered. Column yield was also routinely monitored to ensure quantitative K yield for all other samples processed for K isotope measurement. Our column protocol is similar to the one reported in a recent study that adopted a slightly different HCl molarity of 0.45 mol L⁻¹. HCl of a higher molarity (2 mol L⁻¹) has also been shown to be effective in purifying K from geological samples using bigger columns. ^{66, 80} It is noted that most published studies employ the same or similar cation exchange resin (AG 50W-X8 or -X12) but weak nitric acid as an eluent. 36-38, 62-65, 72, 81-83 Given that most cations have broadly similar behavior on AG 50W resin in HNO₃ and HCl media, 84-87 the two acids should provide similar separation performance upon proper column calibration. The total procedural K blank was <10 ng, which is negligible compared to the typical amount of K processed for a sample ($\geq \sim 20 \mu g$). Our use of relatively large sample sizes was intended to maximize the sample to blank ratio, and to facilitate measurements by the "cold plasma" method for

comparison, although the amount of K mass required by the collision-cell measurement on *Sapphire* MC-ICP-MS is considerably smaller.

2.3 Instrument configurations

Potassium isotope analysis in this study was conducted on a collision-cell MC-ICP-MS "Sapphire" (Nu Instruments, Serial No. SP006) installed in the Department of Earth and Environmental Sciences, University of Minnesota-Twin Cities. This instrument has 16 Faraday cups, 4 secondary electron multipliers (SEM), and 1 Daly detector. All Faraday cups are equipped with 10¹¹-ohm resistors by default, and 13 of them are additionally fit with either 10¹²or 10¹⁰-ohm switchable resistors. The general design of Sapphire MC-ICP-MS has been described in detail in a couple of previous studies.^{70, 72} Briefly, this model features a dual ion path design. The high energy (HE) ion path has an acceleration voltage of 6 kV, and the design is the same as other MC-ICP-MS models from Nu Instruments (e.g., Nu Plasma 2 and 3). Low energy (LE) ion path is unique to Sapphire. It has a lower acceleration voltage of 4 kV and a hexapole collision/reaction cell between the extraction lens and the source defining slit. When the LE path is in use, the ion beam is steered off-axis by a path deflector, followed by deacceleration prior to entering the cell. After passing through the cell, the ion beam is reaccelerated and then deflected on-axis again by a second path deflector to re-enter the rest of beam transfer lens shared with the HE ion path. HE and LE ion paths can be switched through the instrument control software without an instrument shutdown. The collision/reaction cell provides potential advantages for analysis of some isotope systems, such as K, but it may cause some unwanted difficulties for measurement of some other isotope systems, such as lowered ion transmission for light elements and complicated mass fractionation behavior in the cell. The

ġ Zġ

option for a complete bypass of the collision/reaction cell on *Sapphire*, therefore, provides the necessary flexibility that allows users to decide the most suitable mode of operation for the desired analysis.

In this study, K isotopes were primarily analyzed using the collision/reaction cell (i.e., LE path) with a normal RF power of 1300 W at low mass resolution. High-purity (\geq 99.999 %) helium and hydrogen were used as the collision/reaction gases. The removal of Ar-related interferences by the cell allowed the direct monitoring of the 40 K beam. Typically, K concentrations of ~150 to 250 ng mL $^{-1}$ were used during our collision-cell measurements, yielding ion intensity of >150 V on 39 K. This large 39 K beam was collected using a Faraday cup with a 10^{10} -ohm resistor, and smaller 41 K and 40 K beams were measured on Faraday cups with the default 10^{11} -ohm resistors. We also performed some K isotope analysis using the HE ion path with a lowered RF power of 800 W at high mass resolution (i.e., "cold plasma") to check data agreement between the two analytical modes. Due to considerably lower K sensitivity during the "cold plasma" analysis, both 39 K and 41 K isotopes were collected on Faraday cups with 10^{11} -ohm resistors. The large 40 Ar $^{+}$ beam was not measured but absorbed by a "dummy" bucket during "cold plasma" measurements.

A sample–standard bracketing protocol was used during analysis, using NIST SRM 3141a as the bracketing standard. The sample and bracketing standard were always dissolved and diluted in the same batch of 2 % HNO₃ during each analytical session to avoid any difference in acid matrix. An on-peak-zero measurement was made in the same 2 % HNO₃ before each analysis, and the measured intensities were then subtracted from the subsequent sample/standard measurement. Potassium concentrations between the sample and the bracketing standard were typically matched within ~5 % prior to analysis, but varying degrees of concentration mismatch

were tested to better characterize the influence of concentration mismatch on the measured K isotope ratios and to develop a correction method (details in Section 3.4). An Apex Omega HF desolvator and a Teflon nebulizer with a $\sim 100~\mu$ L/min uptake rate, both from Elemental Scientific, were used throughout this study. An Elemental Scientific 2DX autosampler was also used for automated analytical sequences, and each analytical sequence lasted for ~ 12 to 24 hours. The instrument parameters were optimized to give maximum K sensitivity and optimal stability at the beginning of each analytical sequence, and no further tuning was performed once a sequence was started. The detailed instrument, desolvator, and data acquisition settings for K isotope analysis were provided in ESI Table S2.

3. Results and discussion

3.1 The influence of collision/reaction gas flows

Helium (He) and hydrogen (H₂) gases are often used as collision/reaction gases during K isotope analysis, but the response of *Sapphire* collision cell to varied He and H₂ flow rates has not been systematically studied in the past. Here, we assessed different He/H₂ flow rates on K sensitivity and the presence of Ar⁺ and 40 ArH⁺. Sensitivity was monitored by measuring mass-39 and mass-41 intensities in a 200 ng mL⁻¹ high-purity K solution. Ar⁺ was monitored by the mass-40 intensity in K-free clean 2 % HNO₃. Due to relatively high K background in *Sapphire* collision cell (details in Section 3.2), the intensity measured at mass 41 in clean 2 % HNO₃ reflected a sum of 41 K⁺ and 40 ArH⁺. 40 ArH⁺ was estimated by calculating "excess" intensity on mass 41 based on the measured intensity at mass 39 in clean 2 % HNO₃ and an average 41 K/ 39 K ratio of 0.072164 derived from the natural atomic abundance of K, 63 according to the equation Intensity_{MarH+} = Intensity_{mass 41} – 0.072164 × Intensity_{mass 39}.

ġ Zġ

Our results show that a maximum sensitivity of >1000 V per µg mL⁻¹ K can be achieved at different combinations of He/H₂ flow rates; overall, this sensitivity maximum can be reached at a lower H₂ flow as the He flow increases (Fig. 1A). This sensitivity peak shift is consistent with the role of He as a buffer gas;^{88, 89} it promotes interactions between H₂ and Ar and ion transmission through providing additional collisions in the cell. At a constant He flow, K sensitivity typically increases and then decreases as the H₂ flow increases. This trend indicates that H₂ initially facilitates K transmission, probably because of (1) a collision-induced reduction in beam kinetic energy spread, and (2) enhanced removal of ArH⁺ ions (Fig. 1C) that can compete with K ions for transmission. However, as the H₂ flow continues to increase, the number of collisions in the cell becomes unfavorable for K transmission, and, hence, K sensitivity decreases.

Ar⁺ can be reduced to insignificant levels under all tested gas flow rates (Fig. 1B). Although Ar⁺ generally decreases with increasing H_2 flow at a given He flow, this decrease is minor in magnitude and adversely associated with a significant decrease in K sensitivity (Fig. 1A and 1B), so excessive H_2 use provides no benefit for K isotope analysis. We also observed that low H_2 flow rates of <2 sccm (i.e., standard cubic centimeter per minute) could already suppress Ar^+ , but these low H_2 settings were associated with significant $^{40}ArH^+$ (Fig. 1C). As the H_2 flow increases from 2 to 20 sccm, the $^{40}ArH^+$ level decreases from a maximum to a minimum before rising again (Fig. 1C). This trend may reflect a fundamental shift from suppression of plasmaderived $^{40}ArH^+$ through a proton transfer process ($ArH^+ + H_2 \rightarrow Ar + H_3^+$) at lower H_2 flows to increased $^{40}ArH^+$ formation in the collision cell due to an atom transfer reaction ($Ar^+ + H_2 \rightarrow ArH^+ + H$) at higher H_2 flows, based on the known reactions in collision cells. $^{37, 70, 72, 90-92}$ These reactions were further mediated by He. A higher He flow decreases the maximum amount of

plasma-derived ⁴⁰ArH⁺ at low H₂ flows (Fig. 1C), probably caused by He-induced promotion of the proton transfer reaction and dissociation of polyatomic species. As He-induced collisions increase, the chance of the atom transfer reaction in the cell may also increase, leading to increased formation of cell-derived ⁴⁰ArH⁺ at higher H₂ flow rates (Fig. 1C). Based on these results (Fig. 1), our choices of He and H₂ flows, as listed in ESI Table S2, fall within a favorable range that maximizes K sensitivity but minimizes Ar⁺ and ⁴⁰ArH⁺. Although the lowest ⁴⁰ArH⁺ was obtained without He addition (Fig. 1C), we always used He as a precaution to avoid the risk of having an exceedingly large ⁴⁰ArH⁺ beam under certain gas settings.

3.2 Analytical strengths and K background of Sapphire collision cell

Due to nearly complete removal of Ar-related interferences, the collision-cell analysis of K isotopes on *Sapphire* MC-ICP-MS was conducted at the center of K peaks under low-mass resolution with a resolving power of ~300 (Fig. 2), yielding a sensitivity of >1000 V per μg mL⁻¹ K. This represents >2 orders of magnitude improvement in sensitivity, as compared to typical sensitivity achievable using the "cold plasma" method.^{39, 65, 83} The ability for direct analysis of ⁴⁰K by collision cell on *Sapphire* MC-ICP-MS enables new research opportunities, for example, quantification of K isotope fractionation and exchange kinetics in laboratory experiments using the "three-isotope" method. This method has proven valuable in elucidating fundamental behavior of several other non-traditional stable isotope systems in nature, ⁹³⁻⁹⁶ but it has not been applied to K because it would require simultaneous measurements of all three K isotopes. In addition, with appropriate detector configurations that can deal with the low natural ⁴⁰K abundance (e.g., Faraday cup with a 10¹²-ohm resistor or ion counter), the collision cell may also enable high-precision K-Ca geochronology in natural samples.

ġ Zġ

One perceived limitation of the collision cell on Sapphire MC-ICP-MS is its relatively high K background. Typical ³⁹K background measured in clean 2 % HNO₃ is ~2 V in our instrument (i.e., ~2 ng mL⁻¹ K background equivalent concentration). Similar or slightly lower K background levels have been previously reported for other Sapphire MC-ICP-MS.⁷² This high background appears to be limited to K, and we did not observe similarly high background levels for other elements we had tested under the collision cell mode to date, including Ca, Cu, and Fe. The high K background dictates an on-peak-zero correction and imposes a limit on the minimal sample size required for the collision-cell analysis. We normally analyze samples at a K concentration of ~200 ng mL⁻¹ to yield a signal to background ratio above 100, although accurate δ^{41} K results were obtained at signal to background ratios as low as ~50. It is important to recognize that the K sample size (i.e., ~100 µg K) required by the collision-cell analysis on Sapphire under the current background condition is already at least an order of magnitude smaller than sample sizes required by the "cold plasma" method. 39, 65, 83 However, the high K sensitivity and availability of 10¹²-ohm resistors should, in principle, allow for even smaller K sample sizes to be analyzed by the collision-cell mode on Sapphire, if a lower K background level can be achieved.

The high K background under the *Sapphire* collision-cell mode partially results from its very high K sensitivity (~1000 V per μg mL⁻¹ K), but there appear to be other sources that remain unidentified even after our extensive investigations. Currently, we could rule out the sample introduction system (i.e., Apex and peripherals), torch, and cones to be the culprit(s), because thorough cleaning of these components, or replacing them with brand new ones, did not reduce the K background. Interestingly, we observed that the signal to background ratio on our instrument could be altered considerably by changing one or more of Ar gas flows, including

ġ Zġ auxiliary gas to the torch, sweep gas on Apex, and Ar gas to the nebulizer. Typically, as these Ar flow rates increased, the signal to background ratio on our instrument also increased until a plateau was reached, whereas absolute K sensitivity decreased. This observation seems to imply that the K background may result from certain gas-related interactions at the instrument interface, but it is still premature to make any conclusion at this stage.

One possible, but untested, source of high K background may be related to ion extraction processes at the instrument interface. Previous studies, including many based on the first generation collision cell MC-ICP-MS *IsoProbe*, reported that deposition of analyte on the skimmer cone and subsequent extraction of the deposited material by strongly negative potential can contribute to high instrument background for certain elements, particularly, alkali metals. 97
100 This led to development and use of the so-called "soft extraction" that employs a small positive instead of negative potential for ion extraction to mitigate the buildup of analyte ions on the cone (hence background). 38, 97-100 Although the design of *Sapphire* MC-ICP-MS is different from *IsoProbe*, a similar process may occur. Further investigations of the high K background are underway by Nu Instruments.

3.3 Assessment of matrix effects during analysis by the collision cell

3.3.1 Single element doping experiments

We performed a series of cation-doping tests to evaluate matrix effects during K isotope analysis using the collision cell on *Sapphire*. Different cations from high-purity single element standard solutions were added individually in NIST 3141a to make a series of solutions with varied matrix cation to K mass concentration ratios ([matrix cation]/[K] from 0.01 to 0.1). The spiked solutions were then analyzed against pure NIST 3141a. Nine cations, including Na, Mg,

ġ Zġ

- TO SUMPLY OF THE TOTAL STATE OF THE STATE

Al, Ca, Ti, V, Cr, Fe, and Rb, were chosen for the test because (1) they are common major or trace elements in geological samples; (2) they cover masses both lighter and heavier than K isotope masses; (3) some of these elements (V, Cr, Rb) may not be completely separated from K using the popular chromatographic separation protocols based on AG 50W resin, 63, 64, 70 although they are trace elements typically present at concentrations significantly lower than K in natural samples.

Our test results show that elements with masses lighter than K (Na, Mg, and Al) introduce relatively minor effects to K isotope analysis, whereas elements with similar or heavier masses (Ca, Ti, V, Cr, and Rb) can cause more pronounced matrix effects, with the exception for Fe that causes only minor matrix effects (Fig. 3). For NIST 3141a solutions doped with Na or Mg, the measured δ^{41} K values were generally accurate within uncertainty, even at a matrix level up to 10 % of the K concentration (i.e., [Na (or Mg)]/[K] = 0.1). The absence of significant matrix effects associated with Na and Mg also indicated negligible formation of polyatomic species of these two elements that could otherwise interfere with K isotopes, for example, 23 Na 16 O⁺ and 25 Mg 14 N⁺ on 39 K⁺. Aluminum also did not significantly affect the measured δ^{41} K values until a high [Al]/[K] ratio (i.e., 0.1) was present in the solution, which led to a minor but resolvable (~ 0.1 %) shift toward more negative δ^{41} K values relative to the true value. In contrast, elements with masses comparable to, or heavier than, K led to more pronounced matrix effects that degraded data accuracy at comparably low matrix levels, except for Fe (Fig. 3). The presence of ~1-2 % of Ca, Ti, V, Cr, and Rb relative to K started to cause resolvable deviations in the measured δ^{41} K values. The magnitude of the deviation increased with increasing matrix levels, reaching ~0.3 % at the highest [matrix cation]/[K] ratio tested (i.e., 0.1). The effects caused by the presence of Fe are similar to those caused by Al. The Ca-induced matrix effect led

to positive biases in the measured δ^{41} K values, whereas the matrix effects induced by Ti, V, Cr, Fe and Rb caused negative biases. Our results are broadly consistent with a recent study that conducted similar matrix doping tests for K isotope analysis using the collision cell on a different *Sapphire* MC-ICP-MS.⁷⁰ The observed mass-related matrix effects on *Sapphire* broadly conform to previous observations on ICP-MS that heavy matrix elements often cause more pronounced matrix effects on light analytes, ¹⁰¹⁻¹⁰³ implying that the origin of our observed matrix effects may not be uniquely related to the collision cell. The exact origin(s) of such behavior remains debated, and several sources, such as ionization in the plasma, the space charge effect at the plasma interface, and ion collection at detectors, have all been previously proposed.¹⁰¹⁻¹⁰⁵ Testing of these possible sources is beyond the scope of our study.

Compared to the results reported in a previous study, 70 one noticeable difference is that the magnitude of Ca-induced biases is considerably smaller in our study. Our experiments showed a ~0.3 % bias in δ^{41} K at a Ca level of 10 % K (i.e., [Ca]/[K] = 0.1) (Fig. 3). This is the maximum δ^{41} K bias that we observed among three individual Ca-doping tests conducted in different analytical sessions over a period of >2 months. In contrast, the previous study documented a ~0.8 % bias in δ^{41} K at the same Ca level of 10 % K, 70 which is >2 times larger than the bias observed in our experiments. The larger influence of Ca in the previous study was attributed to the formation of 40 CaH⁺ in the *Sapphire* collision cell that directly interfered with 41 K⁺. 70 Two other laboratories that routinely analyze K isotopes using the collision cell on *Sapphire* MC-ICP-MS also indicated non-trivial formation of 40 CaH⁺ that would require either a very low level of Ca presence or correction during the analysis. 72 S To evaluate potential 40 CaH⁺ formation on our instrument, we periodically monitored ion intensity on mass 41 in a series of pure Ca solutions at different concentrations up to 75 ng mL⁻¹ (equivalent to a Ca level of >35 %

K in our cation doping experiments). The ion intensity at mass 41 was found to be always low

ġ Zġ

- TO SUMPLY OF THE TOTAL STATE OF THE STATE

(on average a few millivolts on a 10¹¹-ohm resistor) in pure Ca solutions, and, more importantly, it did not increase with increasing Ca concentrations, suggesting a lack of perceptible ⁴⁰CaH⁺ formation in our instrument. Although the reason for low ⁴⁰CaH⁺ formation in our instrument as compared to other *Sapphire* instruments is unknown, it is certain that the observed Ca-induced matrix effects in our cation doping experiments (Fig. 3) were caused by non-spectral (rather than hydride) interferences. Due to the absence of significant ⁴⁰CaH⁺ formation and adequate removal of Ca in most natural samples by our chromatographic separation, we did not find it necessary to make ⁴⁰CaH⁺ correction during our routine K isotope analysis.

3.3.2 Matrix effects associated with column chemistry

Column chemistry is rarely "perfect" in terms of the absolute purity achievable after the separation, but whether or not the level of matrix elements after column chemistry can affect the intended analysis is instrument dependent. To better characterize the susceptibility of the *Sapphire* collision cell to remaining matrices after column purification, a series of geological reference materials were purified repeatedly through the chromatographic separation up to 3 times, and the purified samples were analyzed after each separation. Seawater and three USGS rock standards of maffect of felsic compositions (BCR-2, AGV-2a, and GSP-2) were used for the test because they cover a diverse range of chemical compositions representative to many geological samples pertinent to stable K isotope research. The test was performed in triplicates for each material. The same reference materials were also analyzed under "cold plasma" conditions on our *Sapphire* MC-ICP-MS after a single-stage purification.

ġ Zġ

Our results show that K isotope analysis by the collision cell on *Sapphire* is more susceptible to matrix effects compared to the "cold plasma" method. The "cold plasma" method obtained accurate δ^{41} K results for all the chosen reference materials after a single-stage purification, whereas the collision-cell method produced erroneous δ^{41} K values that deviated from the consensus values by up to ~0.2 ‰ for rock standards and up to ~2.5 ‰ for seawater (Fig. 4). The deviation was the smallest for GSP-2 that has the highest K content (i.e., 4.48 wt % K) among the chosen reference materials, and the largest for seawater that has the lowest K content (i.e., ~390 µg mL⁻¹ K). At least a two-stage column separation is required to reduce matrix elements in typical geological samples to a level suitable for K isotope analysis by the collision cell on *Sapphire* (Fig. 4).

Sample solutions after each column separation were measured on an iCAP triple-quad (TQ-) ICP-MS (Thermo Scientific) to identify the source of matrix effects during collision-cell measurement. For rock standards, Ti (~2 % K), Al (~4 % K for GSP-2 and AGV-2a, ~10 % K for BCR-2), and Na (~3-15 % K for GSP-2 and AGV-2a) were perceptibly higher in solutions after the first purification, as compared to a level of \leq 1 % K for all these cations in solutions after the second and third purification. For seawater, the sample solution from the first column purification contained high Na of up to twice the K contents, but further purification reduced Na contents to \leq 5 % K. The increased susceptibility of the *Sapphire* collision cell to matrix effects is most likely related to its high ion extraction and transmission efficiency (i.e., ~1000 V per µg mL⁻¹ K), rather than collision cell itself, because our previous work has shown that a single-stage purification was sufficient in yielding accurate δ^{41} K results for BCR-2 and seawater using the collision cell on *IsoProbe* that had much lower K sensitivity (i.e., ~5 V µg mL⁻¹)¹⁰⁶ (Fig. 4). Many single-stage column separation protocols have been reported for stable isotope analysis for

directly adopt these column protocols for collision-cell measurement on Sapphire MC-ICP-MS.

3.4.1 Assessment of concentration mismatch effect during collision cell analysis on Sapphire

It is common practice to match the analyte concentration to the concentration of the

bracketing standard within several percent (often ~5 %) during non-traditional stable isotope

analysis on MC-ICP-MS. 64, 107, 108 because a concentration mismatch may lead to biased isotope

ratio measurements. However, recent studies reported that this concentration mismatch effect is

more pronounced using the collision cell on *Sapphire*, which required more stringent matching

of sample and standard concentrations to be within 1 %.⁷⁰⁻⁷² To test whether or not this previous

observation is common to all Sapphire instruments, we evaluated this concentration mismatch

effect by analyzing a series of NIST 3141a solutions that were intentionally prepared to have K

standard. We routinely performed this concentration mismatch test during each analytical session

concentrations up to ~50 % higher or lower than the concentration used in the bracketing

in the past ~8 months, and the representative results were presented and discussed below.

Before discussing our findings, we first clarify the definition of "concentration

mismatch". The term "concentration mismatch" was used throughout this study to be consistent

with previous studies. 70, 72, 107 but we emphasize that ion intensity mismatch is the fundamental

source for biased isotope measurements. Although, typically, ion intensity is directly related to

the analyte concentration, it can also be affected by other factors, such as the presence of certain

matrix elements, ^{109, 110} and instrument drift (see our results below), which could also result in

biased measurements. In this contribution, we use "concentration mismatch" in a broader sense

K and other metal elements, but our results here indicate that caution needs to be taken to

3.4 Effect of concentration (ion intensity) mismatch and a correction method

ġ Zġ

ġ Zġ to include "ion intensity mismatch" caused by any reason. As a result, our discussion below is always in regard to relative ion intensity (%I), which is quantified by the K ion intensity measured in a sample (I_{sample}) relative to the average K ion intensity of the bracketing standard ($I_{standard}$) measured immediately before and after this sample measurement. This relation is described by the following equation:

$$\%I = \left[\frac{I_{sample}^{i}}{(I_{standard}^{i-1} + I_{standard}^{i+1})/2}\right] \times 100 \text{ (Eq. 1)}$$

where *I* denotes the measured K intensity, and *i* represents the sequence of analysis.

Our results confirm that, indeed, the collision cell mode on *Sapphire* typically shows a strong concentration mismatch effect during K isotope analysis. A \pm ~50 % concentration mismatch could produce a \pm ~1.2 ‰ bias in δ^{41} K using the collision/reaction cell (Fig. 5). This magnitude of bias is comparable to that reported for two other *Sapphire* MC-ICP-MS during collision-cell measurements,^{70,72} but is ~8-time larger than the effect observed on our instrument using the "cold plasma" mode (ESI Fig. S1). This strong concentration mismatch effect poses a major obstacle for high-precision K isotope analysis by the collision cell on *Sapphire*. For example, based on the relation shown in Fig. 5, a ~5 % concentration mismatch between the sample and bracketing standard could cause a ~0.12 ‰ bias in δ^{41} K.

Mitigation of this concentration mismatch effect is critical to achieve highly precise and accurate K isotope analysis. Previous studies were able to overcome this difficulty using one or a combination of the following two methods: (1) optimizing tuning parameters to minimize the concentration mismatch effect during the analysis, or (2) always matching K concentrations between the sample and standard within 1 %.^{70, 72, 82} However, these two approaches have their own limitations. For the first approach, although we were able to reduce the magnitude of the concentration mismatch effect by about a half during the collision-cell measurements in one

ġ Zġ

session in the past ~8 months, we could not reproduce a set of instrument parameters that consistently suppress the concentration mismatch effect on our instrument. For the second approach, although it is straightforward to match K concentrations between the sample and bracketing standard within ~5 %, it gets very tedious and labor intensive to always match concentrations within 1 %. It becomes particularly challenging for automated long analytical sequences (e.g., 12-24 hours), because any subtle difference in evaporation rates in sample and standard solutions can induce gradual divergence in their concentrations over time, even when they are perfectly matched initially. Such difference in evaporation is commonly observed in the laboratory and may result from several reasons, ranging from a less-than-ideal control on laboratory environment to the type and setup of vials and autosampler used during analysis. More importantly, a close concentration match cannot avoid δ^{41} K biases associated with possible instrument drift in ion intensity. As we mentioned above, biased δ^{41} K measurements fundamentally originate from ion intensity mismatch. In the past 8 months, we often observed + ~3 % random drift in ion intensity between two adjacent standard measurements during ~12-24 h automated analytical sequences, and this short-term instrument drift could lead to a \pm ~ 0.1 % spread in the measured δ^{41} K even the same solution was analyzed (Fig. 6), imposing a major limit on the attainable precision.

3.4.2 A correction method for the concentration mismatch effect

Below we will show that the effect of moderate concentration mismatch during K isotope analysis by the collision/reaction cell on *Sapphire* can be corrected, and our correction method is robust in producing accurate δ^{41} K data with a precision of ≤ 0.05 % (2SD). We will describe our correction method first, and then provide evidence that supports the rationale underlying our

ġ Zġ

Our correction method is based an approach previously proposed for analysis of iron isotopes, ¹¹¹ although the previous study did not provide sufficient detail. The correction requires a calibration curve based on analysis of a suite of bracketing standard solutions (i.e., NIST 3141a) intentionally prepared to have a large range of concentration mismatch relative to the concentration of the true bracketing standard during each analytical session. Typically, 4 solutions with concentrations +50 %, +25 %, -25 %, and -50 % of the concentration in the bracketing standard are prepared and analyzed in our routine. The measured δ^{41} K values (δ^{41} K measured) are then fitted against the relative ion intensity (%I) of these solutions using a second-order polynomial function to yield a relation:

$$\delta^{41} K_{measured} = A \times (\%I)^2 + B \times (\%I) + C \text{ (Eq. 2)}$$

where A, B, and C are the constants derived from the curve fit. We found that a second-order polynomial function almost always provided a better fit for the data compared to a linear function. Throughout each analytical sequence, we also calculate $\delta^{41}K$ and %I for each bracketing standard measurement relative to the average of the preceding and subsequent bracketing standard measurements, and then include these data in the curve fit. Incorporation of these data accounts for instrument drift, although the fitted curve is predominantly determined by the data measured for the 4 solutions with large concentration mismatch. An example of our curve fit was illustrated in Fig. 5. Because all solutions analyzed for the calibration curve are made of NIST 3141a and have the same true $\delta^{41}K$ value of 0 ‰, the curve derived from Eq. (2) essentially describes the magnitude of the $\delta^{41}K$ bias as a function of the degree of ion intensity

ġ Zġ

$$\delta^{41}K'_{corrected} = \delta^{41}K'_{measured} - [A \times (\%I')^2 + B \times (\%I') + C]$$
 (Eq. 3)

where δ^{41} K' corrected is the intensity-corrected δ^{41} K value for a sample, δ^{41} K' measured and %I' represent the measured δ^{41} K and relative ion intensity for the sample, and A, B, C are the constants derived from the calibration curve based on Eq. (2). If instrument parameters remained unchanged, the calibration curve stayed valid over the entire duration of an automated analytical sequence of up to ~24 hours on our instrument. As a result, the calibration curve only needs to be established once during each analytical sequence. The calibration curve does vary after re-tuning the instrument with major parameter changes, so our correction should be made on a sequence-to-sequence basis.

A key assumption underlying our correction method is that the response of the measured δ^{41} K bias to ion intensity mismatch in any sample should follow the same response defined by measurements of the suite of bracketing standard solutions with varying concentrations. Otherwise, the calibration curve needs to be established on a sample-to-sample basis, offering no analytical benefits. We found that our assumption is sufficiently good within moderate concentration (ion intensity) mismatch during an analytical sequence. To demonstrate this, we analyzed a series of seawater, BCR-2, and NIST 3141a solutions intentionally prepared to have varied K concentrations up to $\pm \sim 50$ % of the concentration in the bracketing standard. Seawater and BCR-2 were purified through a two-stage column separation prior to the analysis. These two materials were chosen because they have different matrix compositions remaining from column purification (e.g., more Na in purified seawater than BCR-2). Any potential matrix-induced

ġ Zġ

differences in the δ^{41} K bias–%I response should become apparent when comparing the results of these two materials to the result from pure NIST 3141a K solutions.

The test results are shown in Fig. 7A. Data from each of the three materials were fitted using the second-order polynomial function. Overall, the three fitted curves followed a similar trend across a $+ \sim 50$ % range of ion intensity mismatch, although the curves for seawater and BCR-2 gradually deviated from the NIST 3141a-based curve as the degree of intensity mismatch increased. Using the NIST 3141a-based curve as a reference, deviations of seawater and BCR-2 curves from this reference curve can be quantified (Fig. 7B), and they represent δ^{41} K errors that would be introduced during our correction that always applies the NIST 3141a-based calibration curve to samples. Our results showed that although seawater and BCR-2 curves could variably deviate from the NIST 3141a-based calibration curve, possibly due to subtle differences in solution matrices, the magnitude of potential $\delta^{41}K$ errors diminished with decreasing degree of intensity mismatch (Fig. 7B). The potential error is negligible within a reasonably large range of concentration mismatch, for example, <0.04 % within a $\pm \sim 10$ % mismatch and <0.02 % within a $\pm \sim 5$ % mismatch (Fig. 7B). These results indicate that a convenient correction based on a single calibration curve for moderate concentration mismatch is possible. Although this correction does not fully eliminate the necessity to match K concentrations in the sample and bracketing standard, it removes the stringent requirement of having to match concentrations within 1 % during K isotope analysis using the collision/reaction cell on Sapphire. This significantly alleviates the burden of the operator in laboratory and increases the sample throughput. Furthermore, this correction can remove the effect of instrumental ion intensity drift on K isotope analysis, providing an additional analytical benefit that previous approaches do not possess.

ġ Zġ

We routinely applied our correction method to all our K isotope analyses in the past ~8 months. Our δ^{41} K results of a wide range of reference materials were all in excellent agreement with the results reported in literature (ESI Table S1, more details in Section 3.5), demonstrating that our correction method is effective and robust. Uncorrected and corrected δ^{41} K results for UMN-K, seawater, and BCR-2 are shown in Fig. 8 to better illustrate the validity of our correction. These results were collected from 27 to 58 independent analytical sequences spanning a period of ~8 months, and aliquots of seawater and BCR-2 were individually processed through a two-stage column separation every time before analysis. During our routine analysis, we typically aimed at matching K concentrations of the analyte and bracketing standard within $\pm \sim 5$ %, although sessions with slightly larger concentration mismatch of up to $\pm \sim 10$ % can be found due to various reasons, such as intentional tests for our correction method, instrument drift, and differential evaporation in sample and standard vials. As shown in Fig. 8, the uncorrected δ^{41} K data broadly displayed a negative correlation with the relative ion intensity with higher δ^{41} K values corresponding to lower relative ion intensities, but these trends exhibited considerable scatters, showing sequence-to-sequence variability in the δ^{41} K bias-%I response. Although the long-term averages of the uncorrected $\delta^{41}K$ results were accurate for the three materials, the uncorrected data were imprecise with precisions ranging from 0.17 % to 0.24 % (2SD) (Fig. 8). Even if we only consider the δ^{41} K data measured within $\pm \sim 5$ % concentration mismatch, a range commonly targeted during the analysis of many non-traditional stable isotopes on conventional MC-ICP-MS, δ^{41} K precisions were still limited to a level between 0.10 % and 0.15 ‰ (2SD) for the three materials. In contrast, our correction was able to successfully remove the influence of moderate concentration/intensity mismatch over a tested range of $\pm \sim 10 \%$ mismatch (Fig. 8); the corrected δ^{41} K data were accurate and yielded a precision of 0.05 %

ġ Zġ

Several precautions are noted here regarding the application of our correction method. First, although our results show that our correction is effective within a $+ \sim 10$ % concentration mismatch (Fig. 8), it is still recommended to match concentrations between the analyte and bracketing standard within $\pm \sim 5$ % to minimize possible correction errors as shown in Fig. 7. Second, solutions that are used to establish the calibration curve for the correction should cover a large range of concentration mismatch, for example, a $\pm \sim 50$ % mismatch range that we routinely use. A large range in concentration mismatch is more likely to produce a large spread of δ^{41} K values that provides more leverage against analytical uncertainties during the curve fit, and, hence, the δ^{41} K bias-%I response can be better characterized. Third, although we observed that the δ^{41} K bias-%I response was stable over ~12 to 24 hour analytical sequences, and, hence, we only needed to establish the calibration curve once during each analytical sequence. We caution that this may be instrument and laboratory dependent. Individual laboratories should perform tests before deciding the frequency in re-building the calibration curve. Finally, we occasionally observed that the calibration curve did not vary monotonically within the tested -50 % and +50 % relative ion intensity range, and it showed a parabolic shape instead. In this case, a second-order polynomial function was not able to provide a good fit to the data, leading to an erroneous correction. We discovered that the shape of the calibration curve was primarily related to collision/reaction gas flows, and, to a lesser extent, the amplitude of the R frequency applied to the hexapole (i.e., the RF Ref. setting on the instrument). Moderate adjustments to the collision/reaction gas flow rates were always able to help restore a monotonic δ^{41} K bias-%I relation that can be adequately fitted by a second-order polynomial function.

ġ Zġ

- TO SUMPLY OF THE TOTAL STATE OF THE STATE

3.5 Data accuracy, precision, and δ^{41} K values of geological reference materials

Nine reference materials, ranging from pure K solutions to geological materials, were analyzed using the collision cell on *Sapphire* MC-ICP-MS over a period of ~8 months. Pure K solutions were analyzed without purification, and other geological materials were analyzed after a two-stage column purification. All data were corrected for the concentration mismatch effect using the method described in Section 3.4.2. A compilation of our results and data from literature is provided in ESI Table S1.

Our δ^{41} K values measured for all the chosen reference materials are in excellent agreement with the values reported in literature (Fig. 9), validating the accuracy of our measurements. No systematic bias was observed for δ^{41} K data collected using the collision cell and "cold plasma" on our instrument (ESI Fig. S2), including UMN-K that has not been analyzed by other laboratories. Compared to our estimated precision of 0.08 % (2SD) for the "cold plasma" method, the use of *Sapphire* collision cell led to an improved precision of \leq 0.05 % (2SD) (ESCI Table S1), and this precision is among one of the best reported for K isotope analysis in literature (Fig. 9).

Although results for pure K solutions are still limited, δ^{41} K results for geological reference materials are now reported from a good number of laboratories (ESI Table S1), so it is possible to evaluate the degree of interlaboratory data agreement. Currently, seawater and AGV (-1, -2, and -2a) show the best agreement of 0.05 ‰ or better at the 95 % confidence level (ESI Table S1). This agreement also implies that different variants of AGV are homogenous in their K isotope compositions. GSP (-1 and -2), BCR (-1 and -2), and BHVO (-1 and -2) results agree within a range of 0.08 ‰ to 0.10 ‰ at the 95 % confidence interval. The worsened

interlaboratory agreement for these three materials either reflects the current level of interlaboratory reproducibility or subtle heterogeneity among different versions of the same material. Applying the statistics to individual versions of the same material typically yielded slightly better or similar standard deviations, but mean values among different variants of the same material differ by ≤ 0.06 % (Table 3), implying that K isotope heterogeneity between different versions of the material is likely to be small. Thus, the larger interlaboratory disagreement is more likely to reflect the difference in analytical capability of individual laboratories. This shows the need for a continued improvement in analytical precisions across all laboratories involved in K isotope geochemistry research. With the advance and increased availability of collision cell equipped MC-ICP-MS instruments, such as *Sapphire*, *Proteus* and the upcoming collision cell version *Neoma*, a community-level improvement in capability for K isotope analysis is anticipated to accelerate in near future. Our high-precision δ^{41} K results on these reference materials, along with results from other laboratories with comparable precisions, can serve as a useful baseline for future interlaboratory comparisons.

4. Conclusions

ġ Zġ

This study provided a comprehensive assessment of the analytical capability of the latest generation collision cell MC-ICP-MS "Sapphire" (Nu Instruments) for high precision stable K isotope analysis using its collision/reaction cell. We found that He and H₂ gas flows have a major influence on K sensitivity and the ArH⁺ level during collision-cell measurements, and Ar⁺ interference is effectively removed from the cell even at a very low H₂ flow rate. The collision cell mode offers high sensitivity (i.e., 1000 V per μ g mL⁻¹ K at a solution uptake rate of ~100 μ l/min), as well as the ability to directly measure ⁴⁰K that is anticipated to enable new research

ġ Zġ

directions. However, the collision cell on Sapphire is sensitive to the presence of matrix elements during analysis, probably because of the enhanced sensitivity rather than the collision cell itself. This trade-off indicates that effective chromatographic purification is critical for isotope analysis using the collision cell on Sapphire. A major challenge for collision-cell measurements on Sapphire is the strong effect on the measured K isotope ratios from concentration mismatch between the sample and the bracketing standard. The conventional practice of matching sample and standard concentrations within ~5 % is insufficient in ensuring accurate and precise K isotope analysis. However, we demonstrate that the effect of moderate concentration mismatch can be reliably corrected using a convenient method we developed here. Using this correction method, accurate δ^{41} K results with an intermediate precision of $\leq 0.05 \%$ (2SD) can be achieved. Although our method does not fully eliminate the need for concentration matching, it provides critical tolerance for larger concentration mismatch, thereby considerably reducing the burden to the analyst. Also, because our method can correct for the effect of instrument drift in ion intensity and does not require any specific instrument tuning to minimize the concentration mismatch effect, it improves the data quality and significantly increases the sample throughput during collision-cell measurements on Sapphire. Our correction method is expected to be broadly applicable to analysis of other isotope systems. With our improved precision relative to many previous studies, new δ^{41} K results reported here for a range of reference materials can serve as useful baselines for future interlaboratory comparisons.

Author contributions

X.-Y. Zheng was responsible for conceptualization, funding acquisition, investigation, supervision, writing – original draft. X.-Y. Chen, W. Ding, Y. Zhang, and S. Charin were

View Article Online DOI: 10.1039/D2JA00078D

ı	
2	
3	
1	
-	
5	
6	
7	
Ω	
<u>4</u>	
æ 710	
₫0	
<i>भ</i> 1	
33.2	
22	
23	
পূ4	
₹5	
- <u>Ĝ</u>	
ij,	
.년/	
∄8	
49	
ຼືສຸດ	
ug 1	
₹ I	
2 2	
.⊉3	
§ 94	
ğ.	
32	
36	
-2 27	
<u>.</u> 28	
žο	
ر م	
30	
2022 Dewnloaded	
32	
۸	
Published on 27.46 pail 2002 Departused by Tubi New Continues on 12.2022 5.52.01 Pail 8.00 1 2 3 4 5 6 7 8 9 0 1 2 3 4 5 6 7 8 9 0 1 0 6 8 6 9 6 9 7 8 9 0 1 0 6 8 6 9 6 9 6 9 6 9 6 9 6 9 6 9 6 9 6 9	
4	
-3 35	
. 3 6	
- 37	
₽′	

responsible for investigation and writing – review & editing. Y. Gérard was responsible for writing – review & editing.

Conflicts of interest

There are no conflicts to declare.

Acknowledgements

This work is supported by the National Science Foundation under Grant No. 1741048 and a start-up fund from the University of Minnesota to X-Y Zheng. Acquisition of iCAP TQ-ICP-MS was supported by National Science Foundation under Grant No. 1946945 to X-Y Zheng. We would like to thank Michael Jones and Lee Griffiths from Nu Instruments for their technical support in bringing SP006 online during a global pandemic. We also thank Prof. Fang-Zhen Teng at the University of Washington for sharing a suite of NIST solutions used in this study, including NIST 3141a, 193, 918b, and 999c. We thank two anonymous reviewers for their constructive comments and the editor for efficient editorial handling.

References

- R. L. Rudnick and S. Gao, in *Treatise on Geochemistry*, ed. K. K. Turekian, Pergamon, Oxford, 2003, DOI: http://dx.doi.org/10.1016/B0-08-043751-6/03016-4, pp. 1-64.
 - H. Palme and H. S. C. O'Neill, in *Treatise on Geochemistry*, eds. H. D. Holland and K. K. 2. Turekian, Pergamon, Oxford, 2007, DOI: https://doi.org/10.1016/B0-08-043751-6/02177-0, pp. 1-38.
- 3. T. Lyubetskaya and J. Korenaga, Journal of Geophysical Research: Solid Earth, 2007, 112.
- 4. W. F. McDonough and S. s. Sun, *Chemical Geology*, 1995, **120**, 223-253.
- R. D. Jarrard, Geochemistry, Geophysics, Geosystems, 2003, 4. 5.
- S. Y. O'Reilly and W. L. Griffin, in Metasomatism and the Chemical Transformation of Rock: The Role of Fluids in Terrestrial and Extraterrestrial Processes, eds. D. E. Harlov and H. Austrheim, Springer Berlin Heidelberg, Berlin, Heidelberg, 2013, DOI: 10.1007/978-3-642-28394-9 12, pp. 471-533.

4

5

6 7

8

Ę

a0

):25:5202/275 u

Twin Cities on 2 9 2

39

40 41

42

43

44

45 46

47

48

49

50

51 52

53

54

- 735 7. Y. Zhang, Z. Zeng, X. Li, X. Yin, X. Wang and S. Chen, *Geological Journal*, 2018, **53**, 1755-736 1766.
- 737 8. M. R. Palmer, E. Y. Ersoy, C. Akal, İ. Uysal, Ş. C. Genç, L. A. Banks, M. J. Cooper, J. A. Milton and K. D. Zhao, *Geology*, 2019, **47**, 1079-1082.
- 739 9. C. K. Gessmann and B. J. Wood, Earth and Planetary Science Letters, 2002, 200, 63-78.
- 740 10. M. A. Bouhifd, L. Gautron, N. Bolfan-Casanova, V. Malavergne, T. Hammouda, D.
- Andrault and A. P. Jephcoat, *Physics of the Earth and Planetary Interiors*, 2007, **160**, 22-33.
- 743 11. K. Watanabe, E. Ohtani, S. Kamada, T. Sakamaki, M. Miyahara and Y. Ito, *Physics of the Earth and Planetary Interiors*, 2014, 237, 65-72.
- 745 12. Z. Xiong, T. Tsuchiya and T. Taniuchi, *Journal of Geophysical Research: Solid Earth*, 2018, 746 **123**, 6451-6458.
- 747 13. T. T. Isson and N. J. Planavsky, *Nature*, 2018, DOI: 10.1038/s41586-018-0408-4.
- 748 14. D. P. Santiago Ramos, L. E. Morgan, N. S. Lloyd and J. A. Higgins, *Geochimica et Cosmochimica Acta*, 2018, **236**, 99-120.
- 750 15. S. Li, W. Li, B. L. Beard, M. E. Raymo, X. Wang, Y. Chen and J. Chen, *Proceedings of the National Academy of Sciences*, 2019, DOI: 10.1073/pnas.1811282116, 201811282.
- 752 16. J. Sardans and J. Peñuelas, Global Ecology and Biogeography, 2015, 24, 261-275.
- 753 17. C. Zörb, M. Senbayram and E. Peiter, *Journal of Plant Physiology*, 2014, **171**, 656-669.
- 754 18. R. MacKinnon, FEBS Letters, 2003, **555**, 62-65.
- 755 19. K. Lodders, *The Astrophysical Journal*, 2003, **591**, 1220-1247.
- 756 20. B. J. Wood, D. J. Smythe and T. Harrison, *American Mineralogist*, 2019, **104**, 844-856.
- 757 21. P. GEORGES, G. LIBOUREL and E. DELOULE, *Meteorit Planet Sci*, 2000, **35**, 1183-1188.
- 758 22. E. S. Steenstra, N. Agmon, J. Berndt, S. Klemme, S. Matveev and W. van Westrenen, 759 *Scientific Reports*, 2018, **8**, 7053.
- 760 23. M. Humayun and R. N. Clayton, Geochimica Et Cosmochimica Acta, 1995, 59, 2131-2148.
- 761 24. K. Wang and S. B. Jacobsen, *Nature*, 2016, **538**, 487-490.
- 762 25. P. R. Renne, R. Mundil, G. Balco, K. Min and K. R. Ludwig, *Geochimica et Cosmochimica Acta*, 2010, **74**, 5349-5367.
- 764 26. A. Grau Malonda and A. Grau Carles, Applied Radiation and Isotopes, 2002, **56**, 153-156.
- 765 27. K. Kossert and E. Günther, Applied Radiation and Isotopes, 2004, 60, 459-464.
- 766 28. P. R. Renne, C. C. Swisher, A. L. Deino, D. B. Karner, T. L. Owens and D. J. DePaolo,
 767 *Chemical Geology*, 1998, **145**, 117-152.
- 768 29. A. A. Verbeek and Schreine.Gd, Geochimica Et Cosmochimica Acta, 1967, 31, 2125-&.
- 769 30. G. D. L. Schreiner and A. A. Verbeek, *Proceedings of the Royal Society of London. Series*770 *A. Mathematical and Physical Sciences*, 1965, **285**, 423-429.
- 771 31. I. Barnes, E. Garner, J. Gramlich, L. Machlan, J. Moody, L. Moore, T. Murphy and W.
 772 Shields, 1973.
- 773 32. D. Wielandt and M. Bizzarro, *Journal of Analytical Atomic Spectrometry*, 2011, **26**, 366-774 377.
- 775 33. Y. Amelin and R. Merle, *Chemical Geology*, 2021, **559**, 119976.
- 776 34. M. O. Naumenko, K. Mezger, T. F. Nägler and I. M. Villa, *Geochimica et Cosmochimica Acta*, 2013, **122**, 353-362.

4

5

6 7

8

Ę

a0

):25:5202/275 u

Twin Cities on 2 9 2

38

39

40 41

42

43

44

45 46

47

48

49

50

51 52

53

54

55

- 781 37. W. Li, B. L. Beard and S. Li, *Journal of Analytical Atomic Spectrometry*, 2016, **31**, 1023-782 1029.
- 783 38. K. Wang and S. B. Jacobsen, Geochimica et Cosmochimica Acta, 2016, 178, 223-232.
- 784 39. L. E. Morgan, D. P. Santiago Ramos, B. Davidheiser-Kroll, J. Faithfull, N. S. Lloyd, R. M. Ellam and J. A. Higgins, *Journal of Analytical Atomic Spectrometry*, 2018, **33**, 175-186.
- 786 40. H.-O. Gu and H. Sun, *Journal of Analytical Atomic Spectrometry*, 2021, **36**, 2545-2552.
- 787 41. D. P. Santiago Ramos, L. A. Coogan, J. G. Murphy and J. A. Higgins, *Earth and Planetary Science Letters*, 2020, **541**, 116290.
- 789 42. W. Li, X.-M. Liu, Y. Hu, F.-Z. Teng, Y.-F. Hu and O. A. Chadwick, *Geoderma*, 2021, **400**, 115219.
- 791 43. F.-Z. Teng, Y. Hu, J.-L. Ma, G.-J. Wei and R. L. Rudnick, *Geochimica et Cosmochimica Acta*,
 792 2020, **278**, 261-271.
- 793 44. N. X. Nie, X.-Y. Chen, T. Hopp, J. Y. Hu, Z. J. Zhang, F.-Z. Teng, A. Shahar and N. Dauphas, *Science Advances*, 2021, **7**, eabl3929.
- 795 45. B. Tuller-Ross, P. S. Savage, H. Chen and K. Wang, *Chemical Geology*, 2019, **525**, 37-45.
- 796 46. Y. Hu, F.-Z. Teng, T. Plank and C. Chauvel, *Science Advances*, 2020, **6**, eabb2472.
- 797 47. K. Wang, H. G. Close, B. Tuller-Ross and H. Chen, *ACS Earth and Space Chemistry*, 2020,
 798 4, 1010-1017.
- 799 48. H. Chen, X.-M. Liu and K. Wang, Earth and Planetary Science Letters, 2020, 539, 116192.
- 800 49. Y. Hu, F.-Z. Teng and C. Chauvel, *Geochimica et Cosmochimica Acta*, 2021, **295**, 98-111.
- Y. Sun, F.-Z. Teng, Y. Hu, X.-Y. Chen and K.-N. Pang, *Geochimica et Cosmochimica Acta*,
 2020, **278**, 353-360.
- 51. Z. Z. Wang, F. Z. Teng, D. Prelević, S. A. Liu and Z. Zhao, *Geochemical Perspectives* Letters, 2021, **18**, 43-47.
- T.-Y. Huang, F.-Z. Teng, R. L. Rudnick, X.-Y. Chen, Y. Hu, Y.-S. Liu and F.-Y. Wu,
 Geochimica et Cosmochimica Acta, 2020, **278**, 122-136.
- 807 53. W. Li, X.-M. Liu, K. Wang and P. Koefoed, *Chemical Geology*, 2021, **568**, 120142.
- H. Liu, Y.-Y. Xue, G. Zhang, W.-D. Sun, Z. Tian, B. Tuller-Ross and K. Wang, *Geochimica et Cosmochimica Acta*, 2021, **311**, 59-73.
- Y. Jiang, P. Koefoed, O. Pravdivtseva, H. Chen, C.-H. Li, F. Huang, L.-P. Qin, J. Liu and K.
 Wang, *Meteorit Planet Sci*, 2021, **56**, 61-76.
- Y. Jiang, H. Chen, B. Fegley, K. Lodders, W. Hsu, S. B. Jacobsen and K. Wang, *Geochimica et Cosmochimica Acta*, 2019, **259**, 170-187.
- 814 57. X. Li, G. Han, M. Liu, J. Liu, Q. Zhang and R. Qu, *Geochimica et Cosmochimica Acta*, 2022,
 815 316, 105-121.
- 816 58. W. Li, K. D. Kwon, S. Li and B. L. Beard, *Geochimica et Cosmochimica Acta*, 2017, **214**, 1-817 13.
- 818 59. M. Hille, Y. Hu, T.-Y. Huang and F.-Z. Teng, *Science Bulletin*, 2019, DOI: https://doi.org/10.1016/j.scib.2019.09.024.
- 820 60. K. Wang, B. Peucker-Ehrenbrink, H. Chen, H. Lee and E. A. Hasenmueller, *Geochimica et Cosmochimica Acta*, 2021, **294**, 145-159.

4

5

6 7

8

Ę

∄0

):25:5202/275 u

Twin Cities on 2 9 2

39

40 41

42

43

44

45 46

47

48

49

50

51 52

53

54

- 822 61. K. Wang, W. Li, S. Li, Z. Tian, P. Koefoed and X.-Y. Zheng, *Geochemistry*, 2021, DOI: https://doi.org/10.1016/j.chemer.2021.125786, 125786.
- 824 62. K. Hobin, M. Costas Rodríguez and F. Vanhaecke, *Analytical Chemistry*, 2021, **93**, 8881-825 8888.
- H. Chen, Z. Tian, B. Tuller-Ross, Randy L. Korotev and K. Wang, *Journal of Analytical Atomic Spectrometry*, 2019, **34**, 160-171.
- 828 64. Y. Hu, X. Y. Chen, Y. K. Xu and F. Z. Teng, *Chemical Geology*, 2018, **493**, 100-108.
- 829 65. C. Huang, H.-O. Gu, H. Sun, F. Wang and B. Chen, *Spectrochimica Acta Part B: Atomic Spectroscopy*, 2021, **181**, 106232.
- 831 66. X. Li, G. Han, Q. Zhang and Z. Miao, *Journal of Analytical Atomic Spectrometry*, 2020, **35**, 832 1330-1339.
- 833 67. I. C. Bourg, F. M. Richter, J. N. Christensen and G. Sposito, *Geochimica et Cosmochimica Acta*, 2010, **74**, 2249-2256.
- 835 68. F. M. Richter, R. A. Mendybaev, J. N. Christensen, I. D. Hutcheon, R. W. Williams, N. C. Sturchio and A. D. Beloso, *Geochimica et Cosmochimica Acta*, 2006, **70**, 277-289.
- 69. G. Craig, H. Wehrs, D. G. Bevan, M. Pfeifer, J. Lewis, C. D. Coath, T. Elliott, C. Huang, N. S. Lloyd and J. B. Schwieters, *Analytical Chemistry*, 2021, **93**, 10519-10527.
- 839 70. H. Chen, N. J. Saunders, M. Jerram and A. N. Halliday, *Chemical Geology*, 2021, **578**, 840 120281.
- W. Dai, F. Moynier, M. Paquet, J. Moureau, B. Debret, J. Siebert, Y. Gerard and Y. Zhao, Chemical Geology, 2022, **590**, 120688.
- 72. F. Moynier, Y. Hu, K. Wang, Y. Zhao, Y. Gérard, Z. Deng, J. Moureau, W. Li, J. I. Simon and F.-Z. Teng, *Chemical Geology*, 2021, **571**, 120144.
- D. Bevan, C. D. Coath, J. Lewis, J. Schwieters, N. Lloyd, G. Craig, H. Wehrs and T. Elliott, Journal of Analytical Atomic Spectrometry, 2021, **36**, 917-931.
- F. Moynier, Y. Hu, W. Dai, E. Kubik, B. Mahan and J. Moureau, *Journal of Analytical Atomic Spectrometry*, 2021, **36**, 2444-2448.
- K. Wang, W. Li, S. Li, Z. Tian, P. Koefoed and X.-Y. Zheng, *Geochemistry*, 2021, **81**,
 125786.
- 76. A. Makishima, Thermal Ionization Mass Spectrometry (TIMS): Silicate Digestion,
 Separation, and Measurement, Wiley, 2015.
- G. T. F. Wong, T.-L. Ku, M. Mulholland, C.-M. Tseng and D.-P. Wang, Deep Sea Research
 Part II: Topical Studies in Oceanography, 2007, 54, 1434-1447.
- 855 78. T. Yokoyama, A. Makishima and E. Nakamura, *Chemical Geology*, 1999, **157**, 175-187.
- 856 79. F. J. Langmyhr and K. Kringstad, *Analytica Chimica Acta*, 1966, **35**, 131-135.
- 857 80. X. Li and G. Han, Journal of Analytical Atomic Spectrometry, 2021, **36**, 676-684.
- 858 81. E. W. E. Strelow, F. Von S. Toerien and C. H. S. W. Weinert, *Analytica Chimica Acta*, 1970, **50**, 399-405.
- 860 82. Y. Ku and S. B. Jacobsen, *Science Advances*, 2020, **6**, eabd0511.
- 861 83. Y.-K. Xu, Y. Hu, X.-Y. Chen, T.-Y. Huang, R. S. Sletten, D. Zhu and F.-Z. Teng, *Chemical Geology*, 2019, **513**, 101-107.
- 863 84. S. Marsh, J. Alarid, C. Hamond, M. McLeod, F. Roensch and J. Rein, *Cation exchange of 53 elements in nitric acid*, Los Alamos Scientific Lab., 1978.

View Article Online DOI: 10.1039/D2JA00078D

- F. W. Strelow, A. H. Víctor, C. R. Van Zyl and C. Eloff, Analytical Chemistry, 1971, 43, 870-865 85. 866 876.
- 867 86. F. W. Strelow, R. Rethemeyer and C. Bothma, Analytical Chemistry, 1965, 37, 106-111.

2 3

4

5

6 7

8

Ę

a0

):25:5202/275 u

Twin Cities on 2 9 2

39

40 41

42

43

44

45 46

47

48

49

50

51 52

53

54

55

60

- 868 87. F. Nelson, T. Murase and K. A. Kraus, Journal of Chromatography A, 1964, 13, 503-535.
- 869 88. Z. Du and R. S. Houk, Journal of Analytical Atomic Spectrometry, 2000, 15, 383-388.
- 870 89. N. Yamada, J. Takahashi and K. i. Sakata, Journal of Analytical Atomic Spectrometry, 871 2002, **17**, 1213-1222.
- 872 S. D. Tanner, V. I. Baranov and D. R. Bandura, Spectrochimica Acta Part B: Atomic 90. Spectroscopy, 2002, 57, 1361-1452. 873
- 874 M. Iglesias, N. Gilon, E. Poussel and J.-M. Mermet, Journal of Analytical Atomic 91. 875 Spectrometry, 2002, 17, 1240-1247.
- 876 92. G. C. Eiden, C. J. Barinaga and D. W. Koppenaal, Journal of Analytical Atomic 877 Spectrometry, 1996, 11, 317-322.
- 878 93. X.-Y. Zheng, B. L. Beard and C. M. Johnson, Geochimica et Cosmochimica Acta, 2019, 879 **253**, 267-289.
- 880 X.-Y. Zheng, B. L. Beard, T. R. Reddy, E. E. Roden and C. M. Johnson, Geochimica et 94. 881 Cosmochimica Acta, 2016, 187, 102-122.
- 882 95. W. Li, B. L. Beard, C. Li and C. M. Johnson, Earth and Planetary Science Letters, 2014, 883 **394**, 82-93.
- 884 A. J. Frierdich, B. L. Beard, M. M. Scherer and C. M. Johnson, Earth and Planetary Science 96. 885 Letters, 2014, 391, 77-86.
- 886 97. C. Archer and D. Vance, Journal of Analytical Atomic Spectrometry, 2004, 19, 656-665.
- 887 98. J. B. Chapman, T. F. D. Mason, D. J. Weiss, B. J. Coles and J. J. Wilkinson, Geostandards 888 and Geoanalytical Research, 2006, 30, 5-16.
- 889 99. C. W. Magee Jr and C. A. Norris, Geosci. Instrum. Method. Data Syst., 2015, 4, 75-80.
- 890 100. J. Lin, Y. Liu, Z. Hu, W. Chen, L. Zhang and H. Chen, Geostandards and Geoanalytical 891 Research, 2019, 43, 277-289.
- 892 101. S. H. Tan and G. Horlick, Journal of Analytical Atomic Spectrometry, 1987, 2, 745-763.
- 893 102. C. P. Ingle, B. L. Sharp, M. S. A. Horstwood, R. R. Parrish and D. J. Lewis, Journal of 894 Analytical Atomic Spectrometry, 2003, 18, 219-229.
- 895 J. Barling and D. Weis, Journal of Analytical Atomic Spectrometry, 2012, 27, 653-662. 103.
- 896 104. T. W. Burgoyne, G. M. Hieftje and R. A. Hites, Analytical Chemistry, 1997, 69, 485-489.
- 897 105. C. N. Maréchal, P. Télouk and F. Albarède, Chemical Geology, 1999, 156, 251-273.
- 898 106. X.-Y. Zheng, B. Beard, M. Neuman, M. Fahnestock, J. Bryce and C. Johnson, (Under 899 Review).
- 900 107. F.-Z. Teng and W. Yang, Rapid Communications in Mass Spectrometry, 2014, 28, 19-24.
- 901 108. X. Nan, F. Wu, Z. Zhang, Z. Hou, F. Huang and H. Yu, Journal of Analytical Atomic 902 Spectrometry, 2015, 30, 2307-2315.
- 903 X. Y. Chen, T. J. Lapen and H. S. Chafetz, Geostandards and Geoanalytical Research, 109. 904 2017, **41**, 427-435.
- 905 110. P. A. E. Pogge von Strandmann, C. D. Coath, D. C. Catling, S. W. Poulton and T. Elliott, 906 Journal of Analytical Atomic Spectrometry, 2014, 29, 1648-1659.
- 907 111. F. Albarède and B. Beard, Reviews in mineralogy and geochemistry, 2004, 55, 113-152.

- 1 Fig. 1 Influence of different He/H₂ gas flows on K sensitivity (A), Ar⁺ (B), and ⁴⁰ArH⁺ (C). For
- 2 Ar⁺ and ⁴⁰ArH⁺, data were normalized to K sensitivity under corresponding gas settings, so data
- 3 from different settings can be compared directly. (sccm: standard cubic centimeter per minute).

5

- Fig. 2 Typical K peak shapes under collision/reaction cell mode on Sapphire MC-ICP-MS. A
- 6 200 ng g⁻¹ K solution at an uptake rate of 100 μ L min⁻¹ was used for the result shown here. (RP:
- 7 resolving power).

8

- 9 Fig. 3 Results of cation-doping experiments obtained using the collision/reaction cell on
- 10 Sapphire. The shaded horizontal bar indicates the true δ^{41} K value (0 %) of the analyzed solution
- with the estimated precision (0.05 ‰, 2SD).

12

13

- Fig. 4 Results of 4 different reference materials analyzed after sequential chromatographic
- purification using the collision cell and "cold plasma" methods on Sapphire MC-ICP-MS. Our
- previous results measured by *IsoProbe* for BCR-2 and seawater were also shown for comparison.
- 16 Red horizontal dashed lines indicate literature consensus values for these reference materials
- based on our compilation (ESI Table S1).

18

- 19 Fig. 5 Representative results showing the concentration mismatch effect during collision-cell
- 20 measurement on Sapphire. All the analyzed solutions came from the same NIST 3141a stock
- 21 solution but were prepared to have variable K concentrations (red squares). All solutions were
- 22 analyzed against NIST 3141a. The δ^{41} K values calculated for each bracketing standard
- 23 measurement against adjacent bracketing standard measurements were also shown (open
- squares) and included in the curve fit. Incorporation of these data in the curve fit accounts for
- 25 potential effect from the instrument drift in ion intensity.

26

30

- Fig. 6 Representative results showing biased δ^{41} K measurements as a result of the short-term
- random instrument drift in ion intensity during an analytical sequence. All measurements were
- 29 made in the same NIST 3141a solution.

Fig. 7 Results showing responses of the measured δ^{41} K bias to concentration mismatch for three different materials (NIST 3141a, BCR-2, and seawater) with respective regression curves (A). True δ^{41} K value for NIST 3141a is 0 ‰, and true δ^{41} K values for BCR-2 and seawater were based on the results compiled in ESI Table S1. Also shown are the deviations of the sample-specific regression curves from the reference NIST 3141a calibration curve for BCR-2 and seawater, respectively (B). The deviation quantifies potential errors that can be introduced during a sample correction based on the NIST 3141a calibration curve. All solutions were analyzed against NIST 3141a.

Fig. 8 Results showing uncorrected and corrected δ^{41} K values as a function of relative ion intensity for UMN-K, seawater, and BCR-2. Data were collected over multiple individual

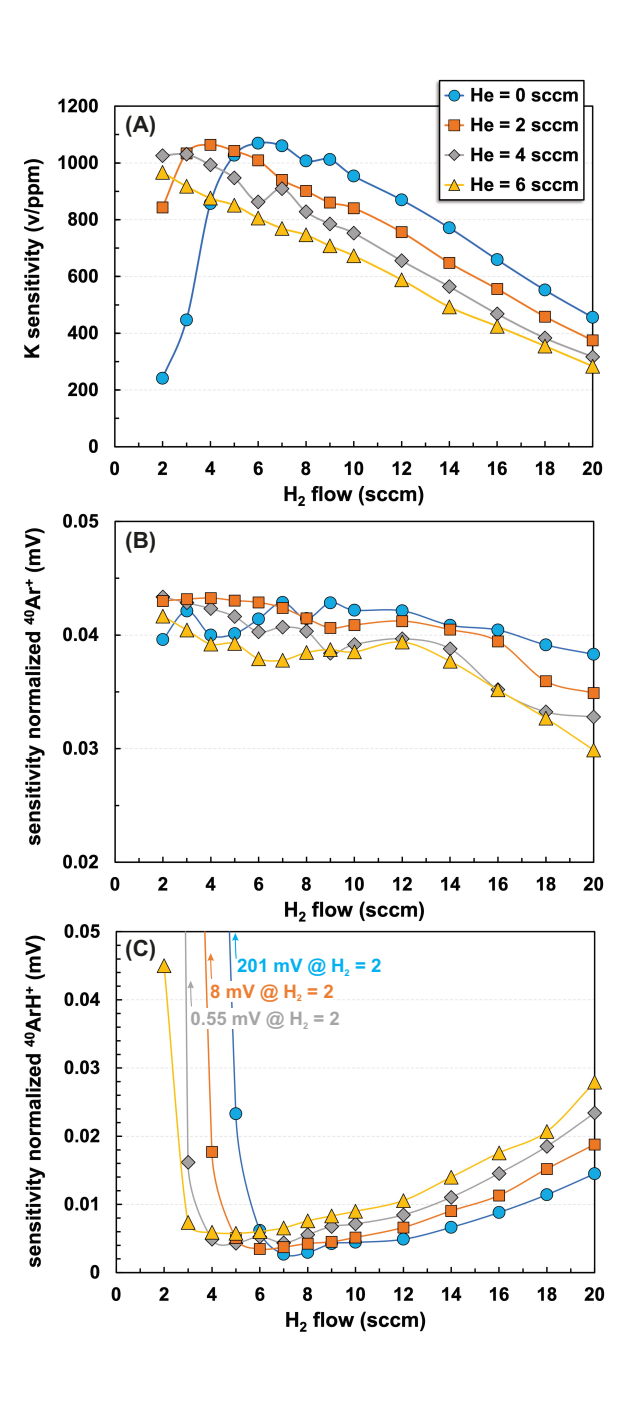
sessions spanning a period of ~8 months.

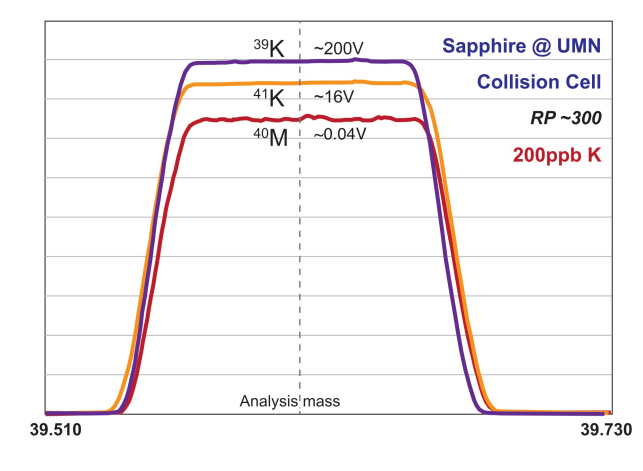
Fig. 9 Our δ^{41} K results for a range of reference materials plotted against literature data reported

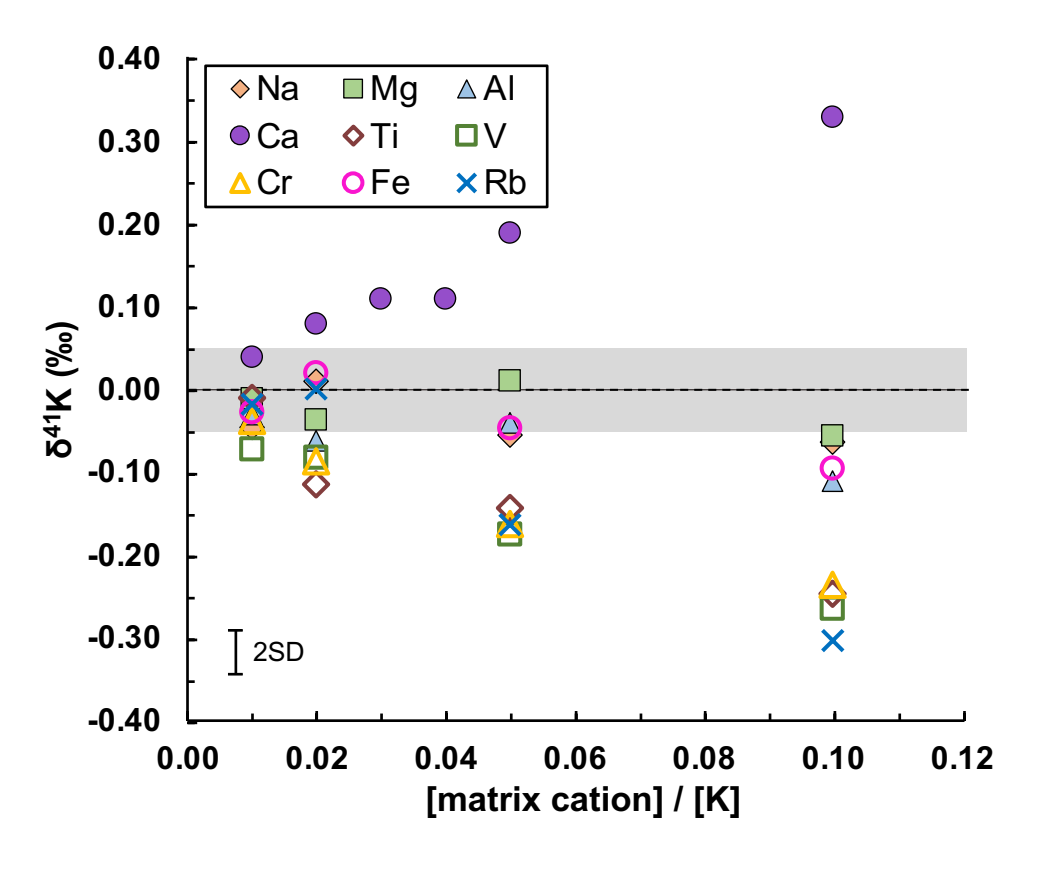
by other laboratories. Different variants of the same material were pooled, and all data are

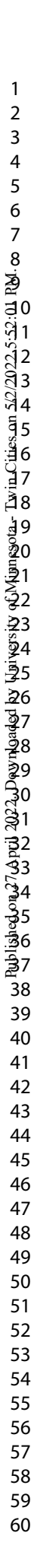
compiled in ESI Table S1.

Journal of Analytical Atomic Spectrometry Accepted Manuscript









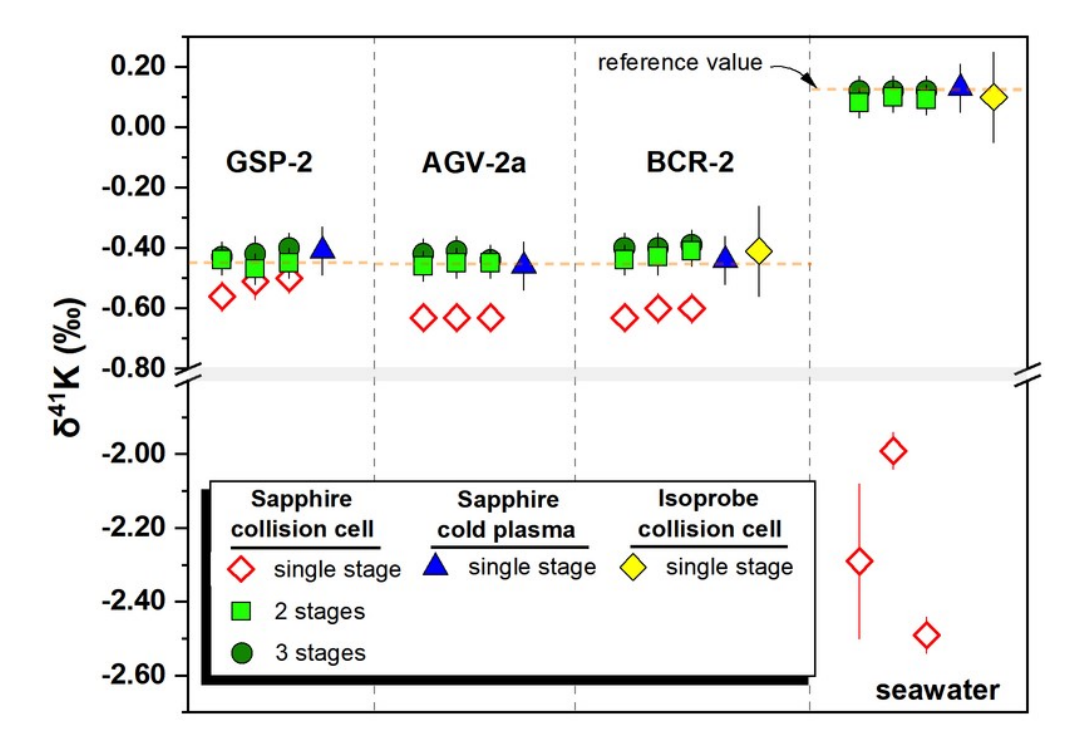


Fig. 4 Results of 4 different reference materials analyzed after sequential chromatographic purification using the collision cell and "cold plasma" methods on Sapphire MC-ICP-MS. Our previous results measured by IsoProbe for BCR-2 and seawater were also shown for comparison. Red horizontal dashed lines indicate literature consensus values for these reference materials based on our compilation (ESI Table S1).

67x46mm (300 x 300 DPI)

ġ Zġ

10:25:57:02/275

Twin Cities on 2 9 2 9

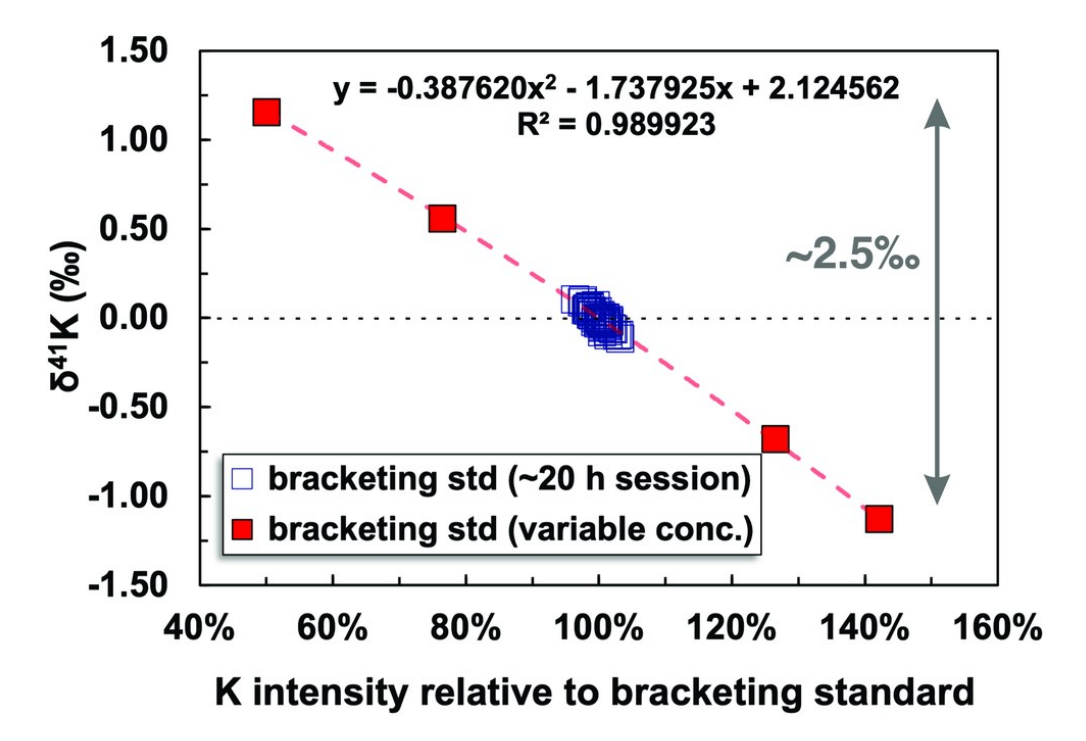


Fig. 5 Representative results showing the concentration mismatch effect during collision-cell measurement on Sapphire. All the analyzed solutions came from the same NIST 3141a stock solution but were prepared to have variable K concentrations (red squares). All solutions were analyzed against NIST 3141a. The δ^{41} K values calculated for each bracketing standard measurement against adjacent bracketing standard measurements were also shown (open squares) and included in the curve fit. Incorporation of these data in the curve fit accounts for potential instrument drift in ion intensity.

82x56mm (300 x 300 DPI)

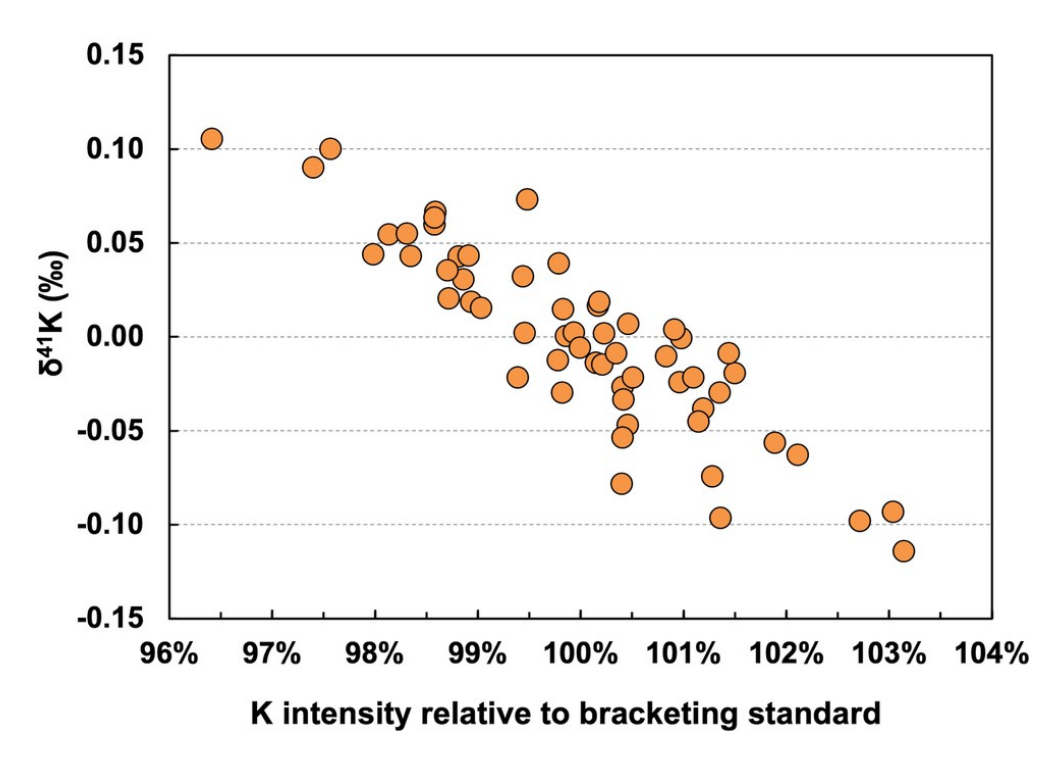
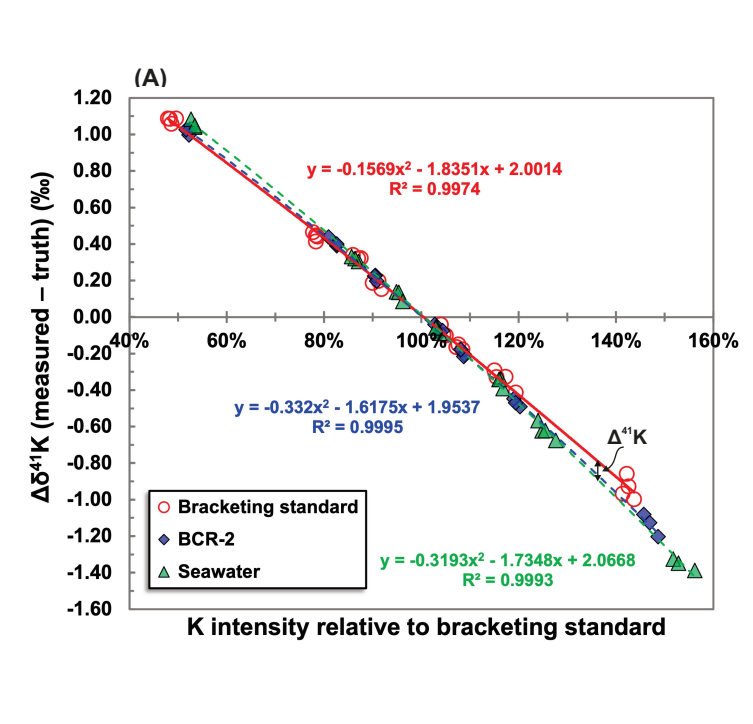
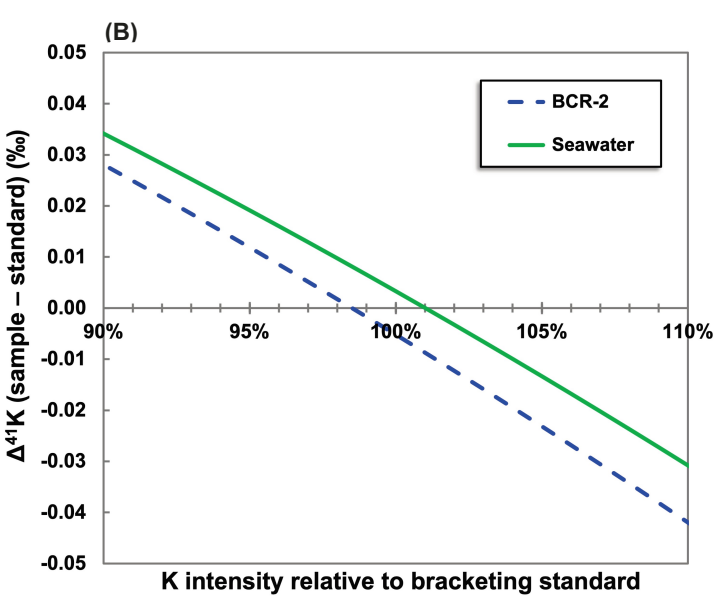


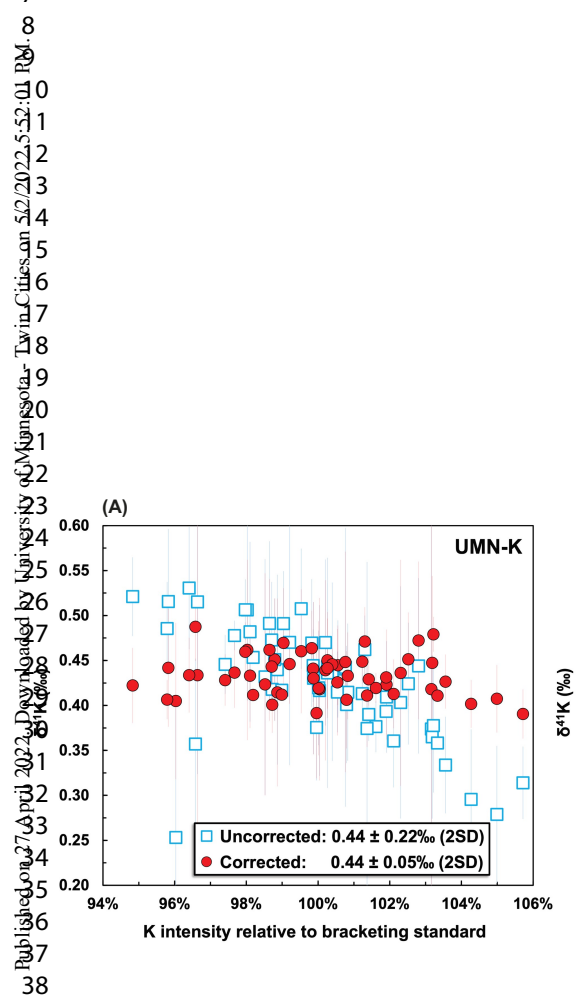
Fig. 6 Representative results showing biased δ^{41} K measurements as a result of the short-term random instrument drift in ion intensity during an analytical sequence. All measurements were made in the same NIST 3141a solution.

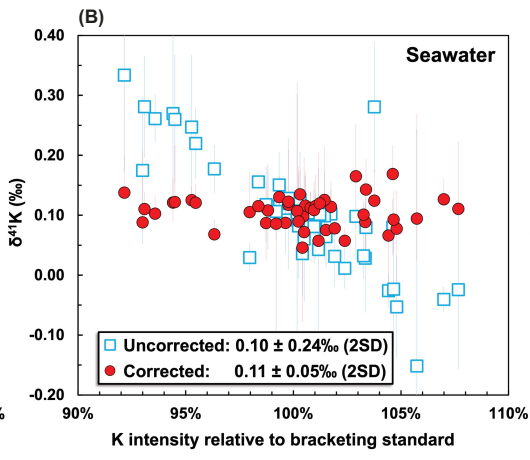
82x57mm (300 x 300 DPI)

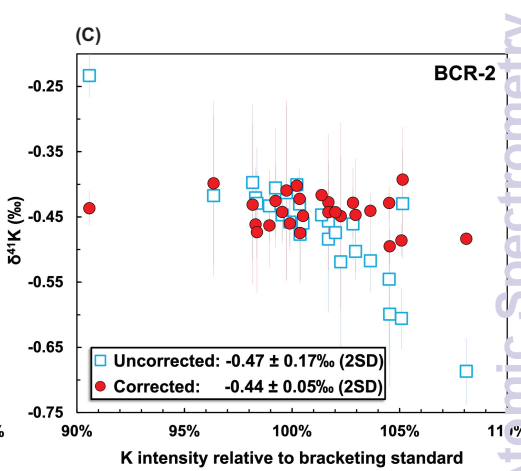
R€.8











8

Fig. 9 Our δ^{41} K results for a range of reference materials plotted against literature data reported by other laboratories. Different variants of the same material were pooled, and all data are compiled in ESI Table S1.

82x41mm (300 x 300 DPI)